Towards a Design Optimization Method for Reducing the Mechanical Complexity of Underactuated Robotic Hands

Frank L. Hammond III, *Member, IEEE,* Jonathan Weisz, Andrés A. de la Llera Kurth,
Peter K. Allen, *Member, IEEE,* and Robert D. Howe, *Senior Member, IEEE*

Abstract—Underactuated compliant robotic hands exploit passive mechanics and joint coupling to reduce the number of actuators required to achieve grasp robustness in unstructured environments. Reduced actuation requirements generally serve to decrease design cost and improve grasp planning efficiency, but overzealous simplification of an actuation topology, coupled with insufficient tuning of mechanical compliance and hand kinematics, can adversely affect grasp quality and adaptability. This paper presents a computational framework for reducing the mechanical complexity of robotic hand actuation topologies without significantly decreasing grasp robustness. Open-source grasp planning software and well-established grasp quality metrics are used to simulate a fully-actuated, 24 DOF anthropomorphic robotic hand grasping a set of daily living objects. DOFs are systematically demoted or removed from the hand actuation topology according to their contribution to grasp quality. The resulting actuation topology contained 22% fewer DOFs, 51% less aggregate joint motion, and required 82% less grasp planning time than the fully-actuated design, but decreased average grasp quality by only 11%.

I. INTRODUCTION

THE design of robotic hands for dexterous grasping and manipulation has historically been an exercise in biomimicry, with many of the most well-recognized and successful solutions taking on kinematically complex, fully actuated anthropomorphic forms [1,2] (Fig. 1). The biomimetic design approach, in principle, is a sensible one in that it seeks to emulate the form and functionality of the human hand, which possesses a proven capability to perform complex grasping and manipulation tasks on a wide variety of objects in unstructured environments [3]. In practice, however, fully-actuated anthropomorphic robotic hand solutions have proven prohibitively expensive and difficult implement due to (1) the requisite mechanical sophistication of their actuation topologies, (2) the need for high-fidelity sensing, and (3) the demand for advanced control methods necessary for such highly-articulated manipulation systems [4]. In order to realize inexpensive, adaptive robotic grasping solutions, a favorable balance between mechanical complexity and grasp robustness must be achieved.

Fig. 1. A 24 DOF fully actuated robotic hand model grasping a mug using both an anthropomorphic and a non-anthropomorphic finger configuration.

Actuation topologies – the kinematic arrangements and mechanical couplings of actuation systems - are integral to the efficiency and versatility of dexterous robotic hand solutions but are generally the most challenging and expensive design components to implement. Fully actuated anthropomorphic robotic hands have historically made liberal use of actuators to achieve individual control of each degree of freedom (DOF) – previously thought to be an essential feature - but have suffered from the computational cost of sensing and control, and the expense and technical difficulty of hand construction. These issues catalyzed the migration from fully actuated hands to traditional underactuated robotic hands, which employ rigid joint coupling in order to reduce actuator requirements, decrease production costs, and avail more tractable sensing and control schemes [5]. Recent efforts to merge underactuation with compliant mechanisms have permitted further simplification of robotic hand actuation topologies while affording passive adaptation to unstructured settings and robustness against sensing errors [6].

The progressive evolution of actuation technologies, coupled with the design and control insights derived from the study of human grasp taxonomies [7] and postural hand

synergies [8], has fostered the development of computationally efficient grasp planning methods [9] and the creation of cheap, effective, highly underactuated compliant hand solutions [6]. However, the dependence of these solutions on compliant mechanical features rather than computational implements has recast the problem of robotic hand design into an exercise in mechanical parameter tuning. The new design space of underactuated compliant hands, which now includes joint stiffness, stiffness ratios [10], and tendon-placement parameters [11], is too vast to be searched exhaustively and, to complicate design matters further, the nature and role of the reduced actuation topologies must be carefully balanced against mechanical feature selection.

This paper constitutes our first steps in characterizing and understanding the tradeoff between robotic hand design complexity and grasp quality. We present a computational framework for reducing the mechanical complexity of actuation topologies used in underactuated compliant robotic hands without sacrificing grasp robustness. This framework employs a top-down, data-driven design approach that systematically demotes or removes DOFs from a fully-actuated robotic hand model based upon their effective contribution to grasp robustness. We use this framework to impose actuation topology reductions ATRs over several design iterations to produce a robotic hand solution with lower mechanical complexity and greater amenability to grasp planning than a fully actuated hand, but with comparable levels of grasp robustness. We then use grasp solution data from the reduced actuation topology to help inform the integration of passively compliant DOFs and the coupling of individual DOFs for the purpose of underactuation.

II. ACTUATION TOPOLOGY REDUCTION FRAMEWORK

The robotic hand actuation topology reduction problem presented here works to improve actuation efficiency by demoting (reducing the motion range) or eliminating DOFs that have a marginal impact on the achievement of grasp robustness. In theory, removing DOFs that are seldom used or have low correlation to grasp quality should reduce the mechanical complexity and, by extension, the cost of a hand design solution, without compromising performance. This reduction should also markedly decrease the size of the grasp configuration space, abating the computational cost of motion planning and control required for such highly articulated systems. The ATR problem is conceptually straight-forward, but the degree to which it affects robotic hand design cost and functionality is heavily dependent upon the formulation of the design framework.

A. Design Objective of ATR

The primary goal of ATR is to find the *minimum complexity* topology necessary to achieve grasp robustness over a specific task set. A *minimum complexity* actuation topology can be defined as one that:

- Minimizes the number of active DOFs needed to actuate the robotic hand during object grasp acquisition.
- Reduces aggregate range of motion (the sum of all hand DOF motion ranges) needed to meet grasp quality specifications, thus eliminating 'wasted' motion range.
- Reduces total DOFs by removing less useful ones and coupling those having highly correlated motion.

These criteria are not necessarily correlated as measures of actuation topology fitness. For example, an actuation topology solution with fewer DOFs may require larger motion ranges to conform to various object morphologies. To avoid this ambiguity in performance criteria, we frame topology reduction as a performance thresholding problem. Rather than optimizing actuation topology fitness with respect to linearly weighted design criteria, we systematically demote or remove robotic hand DOFs until grasp quality falls below a certain 'acceptable' performance threshold. We then use these criteria to characterize the resulting topology solution, and to distill the relationship between design parameters and grasp robustness.

B. Computational Design Optimization

This study relies on the following physical assumptions and modeling simplifications to ensure the computational tractability of robotic hand grasp simulations.

- *Design space culling*: ATR parameters will include only DOF motion ranges, and not morphological parameters such as link length, or mechanical parameters such as compliant joint stiffness and actuator torque.
- *Mechanics Assumptions*: Grasp simulations consider only basic, quasi-static physics for object grasp acquisition, excluding more complicated physics such as soft contact mechanics and compliant flexure joints.
- *Object-Specific Grasp Features*: Grasp quality metrics consider only geometric characteristics (contact point distribution) and gross mechanics (force-closure) of hand-object interaction, and do not encode the cognitive mechanisms humans use to identify object affordances or mechanical wrenches required for object use.
- *Grasping, not Manipulation*: This focuses exclusively on the acquisition of power grasps, not pinch/fingertip grasps associated with in-hand object manipulation. Manipulation mechanics are not well understood, and are not fully supported by current simulation software.

Although these assumptions and simplifications obviate some important insights into the influence of actuation topology on grasp mechanics, they are essential to the tractability of this simulation-based design framework. We assert that the formulation of this framework is appropriate for proof of the ATR concept and its efficacy, and will serve as a baseline for more thorough treatments of underactuated compliant robotic hand design in the future.

The grasp simulations conducted for this study are performed using *GraspIt!*, an open-source software package developed at the Columbia Robotics Lab [12,13]. *GraspIt!* provides a comprehensive framework for the kinematic and mechanical modeling of robotic hands, graspable objects, and environmental obstacles, and contains an assortment of grasp planning and analysis tools essential for robotic hand design evaluation. This section describes robotic hand and object models used in this study, and the settings used for grasp planning, acquisition, and evaluation in *GraspIt!*.

A. Fully-Actuated Robotic Hand Model

The initial, fully actuated robotic hand model contains 24 active, revolute DOFs. These DOFs are distributed evenly across four kinematically identical digits, such that each has six DOFs, listed in Table I and illustrated in Figs. 2 and 3.
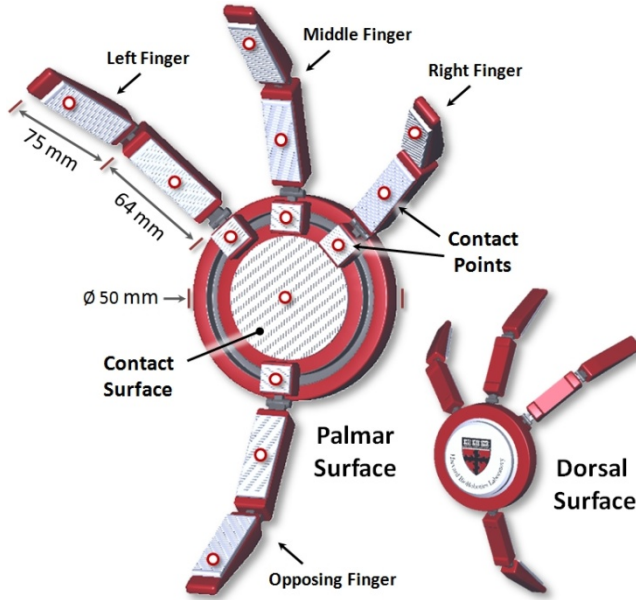

Fig. 2. The initial 24DOF fully-actuated robot hand model, with major dimensions, contact surface locations, and finger designations.

The choice of the robotic hand DOFs and their initial configurations is inspired partly by the human hand, and partly by design solutions developed in research. Distal and proximal flexion/extension DOFs and the finger base rotation DOFs are a common trait among biological and artificial hand designs, and are kept here as a compulsory element in the hand design space. Distal and proximal link twist DOFs are uncommon among rigid hand solutions and human hands, but have demonstrated utility in promoting conformation to object curvature in compliant hands [6].

Finger abduction DOF about the palm center allows motion comparable to human finger abduction (spreading apart of the fingers), but the kinematics defined here allow for a non-anthropomorphic range of abduction. This DOF has shown utility in industrial robot hand solutions and, in this case, allows the robotic hand to assume a variety of

finger-palm configurations, including a 3-1 anthropomorphic configuration, a 2-2 opposing pair configuration similar to the Harvard Hand [6], and a spherical configuration. Adding this DOF to the hand configuration space will provide insights on the importance of gross finger positioning in achieving grasp robustness, and will also help elucidate the value of non-anthropomorphic actuation topologies.

TABLE I
INITIAL HAND JOINT POSITIONS AND MOTION RANGES

Robotic Finger DOF	θ_{ini}(°)	θ_{min}(°)	θ_{max}(°)
θ_1: Finger Abduction			
Left finger	-45	0	-180
Middle finger	0	0	0
Right finger	45	0	180
Opposing finger	180	135	225
θ_2: Base Rotation	0	-45	45
θ_3: Proximal Flexion	30	0	130
θ_4: Proximal Twist	0	-45	45
θ_5: Distal Flexion	30	0	140
θ_6: Distal Twist	0	-45	45

All angles are valued with respect to the axes and zero positions shown in Fig. 3.
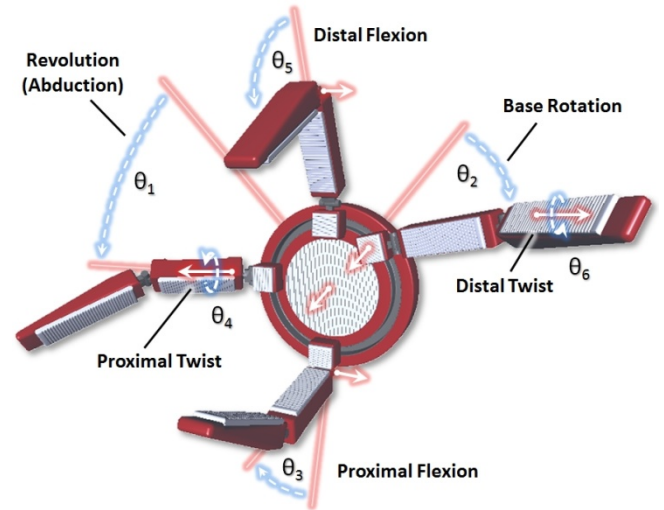

Fig. 3. Robotic hand DOFs. Finger abduction is measured against the middle finger's initial position. Base rotation angles are measured with respect to radial lines drawn from the palm center. Flexion/extension and twist DOFs are measured with respect to angles at which distal and proximal link contact pads are parallel to the palm contact pad.

B. Graspable Objects and Structured Obstacles

The design of dexterous robotic hands is largely focused on human environments, both domestic and industrial, which contain objects of various size, shape, and mechanical properties. Along these lines, we selected eight representative daily living objects from the object set characterized in [14] and assigned the corresponding mass and surface friction properties. Because this research focuses on dexterous object grasping, and not manipulation, only objects that require power grasps (cylindrical, spherical, and pad) were chosen. These objects are shown in Fig. 4.

Fig. 4. The set of daily living objects used in this study. These objects include a two-liter bottle, an aerosol spray can, a glass beverage bottle, a coffee cup, a bowl, a doorknob, a stapler, and a wrench. The dimensions of these objects are in close agreement with objects listed in [14].

The quality metrics currently used in grasp planning [15] are driven by the mechanical properties and shapes of target objects, and the dynamics of the interactions between robotic hands and objects. These metrics do not, however, incorporate knowledge of an object's intended use which, for humans, naturally eliminates certain hand configurations and object contact areas from consideration. To address this, we developed a set of structured grasp obstacles for the target objects. These obstacles serve to prevent grasp solutions that would, by human visual inspection and mechanical intuition, appear to diminish object utility. Figure 5 shows a coffee cup with a structured obstacle that prevents contact with the bottom and inner surfaces.

Fig. 5. Coffee cups are not usually grasped from their bottom or inner surfaces, thus the corresponding obstacle prevents access to those areas.

C. Measuring Grasp Robustness

Several methods have been proposed for the assessment of grasp quality in simulation. These range from force-based metrics that measure robustness against disturbance wrenches [16, 17] to geometry-based methods that measure hand-object contact topology [18, 19] and degrees of force-closure [20]. We use two metrics to measure grasp quality:

- *Hand contact energy*: used in grasp planning to achieve hand preshapes likely to result in well-distributed hand object contact points during grasp acquisition. Sums the distance between predefined robotic hand contact points and the object surface, and the angular differences between hand contact normals and the closest object surface normals. Low contact energy means good hand-object surface contact point alignment [21].

- *Epsilon quality*: after the completion of grasp planning and acquisition determine degree of force and form closure achievable from a given grasp preshape. Determines the ability of a grasp to resist external wrenches applied to the grasped object. Higher epsilon quality means greater force closure.

Hand contact energy serves as a basis for eliminating from consideration pregrasps that are unlikely to result in successful grasps, but it should be noted that hand contact energy for a given robotic hand preshape does not necessarily correlate with epsilon quality at grasp acquisition. Preshapes with high hand contact energy (desired contacts are far from object surface) may result in high epsilon quality (robust grasps), while low contact energy preshapes may result in poor epsilon quality. The latter occurrence, according simulation results, is far more common. For this reason, both hand contact energy and epsilon quality are employed in grasp robustness assessment.

D. Planning and Optimizing Grasps

Grasp planning and optimization for high dimensional systems such as the 24 DOF robotic hand is challenging for several reasons. First, the hand configuration space - consisting of both finger postures and wrist position and orientation - is very large and complex, and must satisfy multiple motion constraints including the avoidance of object, obstacle, and self collisions, and adherence to joint limit specifications. Second, the computation of analytical gradients for optimization is often very difficult, if not completely intractable. This is due in large part to the high sensitivity of grasp quality functions to small changes in individual DOF positions. Third, this study does not assume *a priori* knowledge of postural synergies or eigengrasps for the robotic hand model [9], thus there is no reduction of configuration space dimensionality before optimization. While this fact is not innately problematic, in this case it serves to further exacerbate the challenges of gradient computation and configuration space constraint satisfaction.

These computational roadblocks are mitigated by using simulated annealing as the optimization method. This stochastic search method is particularly useful in cases where objective function gradients are difficult to compute, or when several local function minima exist. The utility of simulated annealing, however, entails greater computational cost. As evidenced in previous research, also conducted using *GraspIt!* [21,22], eigengrasp-based grasp planning using simulating annealing requires on the order of 100,000 search iterations to reach satisfactory grasp energy levels. Our own grasp planning tests, using hand contacts as the energy formulation, show that satisfactory grasp energy levels for the 24 DOF robotic hand can be achieved reliably using a maximum count of 125,000 iterations.

IV. ACTUATION TOPOLOGY REDUCTION ALGORITHM

The ATR algorithm is comprised of three main steps: 1) the *GraspIt!* simulation of the 24 DOF robotic hand grasping the representative daily living objects, 2) the ranking of grasp solutions by quality metrics and statistical analysis of robotic hand motion, and 3) redesign of the actuation topology by the demotion or elimination of ineffectual DOFs. This section describes the formulation of these steps.

A. Grasp Planning and Acquisition

At each iteration of the algorithm, the most recent instantiation of the 24 DOF robotic hand model is simulated grasping each of the objects in the representative object set. Each grasp simulation is composed of 1) a planning phase during which a grasp preshape is assumed, followed by 2) a grasp acquisition phase during which the grasp quality afforded by the preshape is measured. Grasp planning involves searching the hand configuration space using simulated annealing until the grasp preshape with minimum contact energy is found. Grasps are acquired using *GraspIt!*'s "Autograsp" function, which first drives the preshaped hand toward the target object until initial contact, then closes the hand according to predefined default DOF velocities. To prevent undesired finger twisting motions during grasp acquisition, only the flexion-extension DOFs are given non-zero default velocities. Distal flexion-extension DOF velocities are set to 50% of proximal flexion-extension DOFs to promote more efficient grasp acquisition.

B. Pruning Grasp Solutions

Because this algorithm uses simulated annealing to search a vast grasp solution space, we expect a large variance in the quality of grasp solutions. To ensure that ATRs are based only on high-quality solutions, we simulate a large number of grasps and prune from that solution set the grasps which are of unacceptable quality. At each design iteration we simulated 100 grasps per object and ranked the solutions first according to contact energy, and second according to epsilon quality. Those grasps which resulted in a negative epsilon value, indicating lack of any robustness against external wrenches, were eliminated from the solution set.

We chose from each object's remaining grasp solutions the top 10 grasps according to contact energy and epsilon quality, and we statistically analyzed these 80 total grasps (10 from each of the 8 objects) to determine which robotic hand DOFs would be modified or eliminated.

C. Statistical Basis of Actuation Topology Reduction

1) Demoting DOFs Least Important to Robustness

After grasp simulation and solution pruning, the solution data was analyzed to determine which DOFs contributed least to the achievement of robust grasps across the object set. Each DOF's level of contribution to grasp robustness was measured by utility index g_{util}, defined as the ratio of the standard deviation of its solution values, $\mathbf{x}_{DOF}$, to its total motion range (1). This index quantifies how efficiently a DOF's motion range was utilized during grasp simulations.

$$g_{util} = \frac{\sigma(\mathbf{x}_{DOF})}{\max(\mathbf{x}_{DOF}) - \min(\mathbf{x}_{DOF})} \qquad (1)$$

The four robotic hand DOFs with the lowest utility indices are "demoted" to a smaller motion range. No restrictions are imposed on the distribution of DOF demotions – all demotions can occur on the same digit, if necessary. However, the total number of four allows demotions to be spread evenly over all digits if a particular DOF type (proximal twist, distal flexion, base rotation, etc.) exhibits low utility across all digits for a given design iteration.

The graduated motion range scale used to demote DOFs is shown in Table II. A DOF is demoted when its motion range is decreased to the lower limit of the scale range that its standard motion deviation falls into. For example, if $\sigma_1(\mathbf{x}_{DOF})$ of a demoted DOF is equal to 35° (within Level 3), then its new motion range will be reduced to 30° - the lower limit of level 3. If a DOF is demoted while at the lowest level of the motion scale, Level 1, it is eliminated from the actuation topology by assignment of a zero-motion range.

TABLE II
GRADUATED DOF MOTION RANGE DEMOTION SCALE

Level	DOF Deviation (°)	Demoted Range (°)
4	$\sigma(x_{DOF}) \geq 45$	±45 (90)
3	$45 > \sigma(x_{DOF}) \geq 30$	±30 (60)
2	$30 > \sigma(x_{DOF}) \geq 15$	±15 (30)
1	$15 > \sigma(x_{DOF}) \geq 0$	0 (locked)

Any DOF whose standard deviation falls within Level 1 is made rigid by assignment of a zero motion range.

2) Actuation Topology Design Protocol

After the four DOFs with the smallest utility indices are demoted, their initial positions are set to the mean of their solution values for that iteration. The new range of motion is then fit to the mean such that half of the range exists in each motion direction. For a DOF mean μ_x and a motion range of 90°, the absolute limits will be $\mu_x \pm 45°$.

D. Reduction Algorithm Stopping Criteria

The ATR algorithm terminates once the percentage of grasp solutions having hand contact energies less than 15.00 falls below 60%. Below this point, we assume that the current robotic hand design cannot reliability facilitate grasp robustness over the representative object set.

V. RESULTS

The ATR algorithm ran for seven iterations, after which the grasp energy stopping criteria was reached. The sixth design iteration yielded the *minimum complexity* solution. Table III lists DOF demotions that were imposed during the ATR algorithm. Each table column represents a hand DOF, and each row represents a design iteration. Bold numbers indicate that a DOF was demoted to the lower limit of the corresponding motion range level (refer to Table II).

Design Iteration	LEFT						MIDDLE						RIGHT						OPPOSING					
	θ_1	θ_2	θ_3	θ_4	θ_5	θ_6	θ_1	θ_2	θ_3	θ_4	θ_5	θ_6	θ_1	θ_2	θ_3	θ_4	θ_5	θ_6	θ_1	θ_2	θ_3	θ_4	θ_5	θ_6
Original	4	4	4	4	4	4	1	4	4	4	4	4	4	4	4	4	4	4	4	4	4	4	4	4
1	4	2	4	4	4	4	1	2	4	4	4	4	1	2	4	4	4	4	4	2	4	4	4	4
2	4	2	4	4	4	1	1	2	4	4	4	1	1	2	4	4	4	1	4	2	4	4	4	1
3	4	2	3	4	4	1	1	2	4	4	4	1	1	2	3	4	4	1	4	2	3	4	4	1
4	4	2	3	4	3	1	1	2	3	4	3	1	4	2	3	4	4	1	4	2	3	4	4	1
5	4	2	2	4	3	1	1	2	3	4	2	1	1	2	3	4	4	1	4	2	3	4	4	1
6*	4	2	1	4	3	1	1	2	3	4	2	1	1	2	2	4	3	1	4	2	3	4	3	1
7	4	2	1	4	2	1	1	2	3	4	2	1	1	2	2	4	2	1	4	2	2	3	3	1
Final	4	2	1	4	2	1	1	2	3	4	2	1	4	2	2	4	2	1	4	2	2	3	3	1

Columns represent robotic hand DOFs, rows are design iterations, numbers within columns indicate current motion range level, and bold numbers indicate the demoted motion range. Motion range levels at demotion are: **4** = 90°, **3** = 60°, **2** = 30°, and **1** = 0°.

The resulting robotic hand design, shown in Fig. 6, contains five fewer DOFs than the original hand, and has an aggregate motion range of 19.39 radians, down from 44.87 radians. This hand has an initial configuration comprised opposing finger pairs, with one pair having larger finger separation than the other. The finger abduction allowed by the new actuation topology permits the assumption anthropomorphic hand postures from the opposing pair configuration, but biases the robotic hand toward grasps that are hand-symmetric, with one pair of fingers on opposite sides of an object's major axis (Fig. 7). This major axis grasp bias agrees with recent work on grasp planning [22].

One noticeable feature in the final hand design is the absence of distal link twist DOFs, which were demoted directly from their initial motion range to a zero-range due to small motion deviations (<15°). These DOFs may have some value as compliant joints, but their limited contribution to grasp quality did not warrant full actuation. The elimination of this DOF agrees with the kinematics of human hands and of most robotic hands.

Another salient design feature is the prominence of the finger abduction. This DOF, cited in neuroscience literature as being critical to the principal components of human postural synergies [8], plays an equally important role in this robotic hand. Finger abduction was the only DOF type not demoted below motion range level 4 during topology reduction, and had the largest variance throughout the topology reduction process.

The total simulation time required for grasp planning decreased by 82% after ATR, confirming the hypothesis that smaller configuration spaces reduce computational costs (Fig. 8). Planning time suddenly increased after iterations two and six because a DOF had been eliminated from the hand, and the resulting searchable configuration space, though smaller, contained fewer viable solutions initially. Contact energy increased by 11%, signifying a decrease in grasp quality, while the percentage of solutions with sufficiently low contact energy dropped by 12% (Fig. 9)
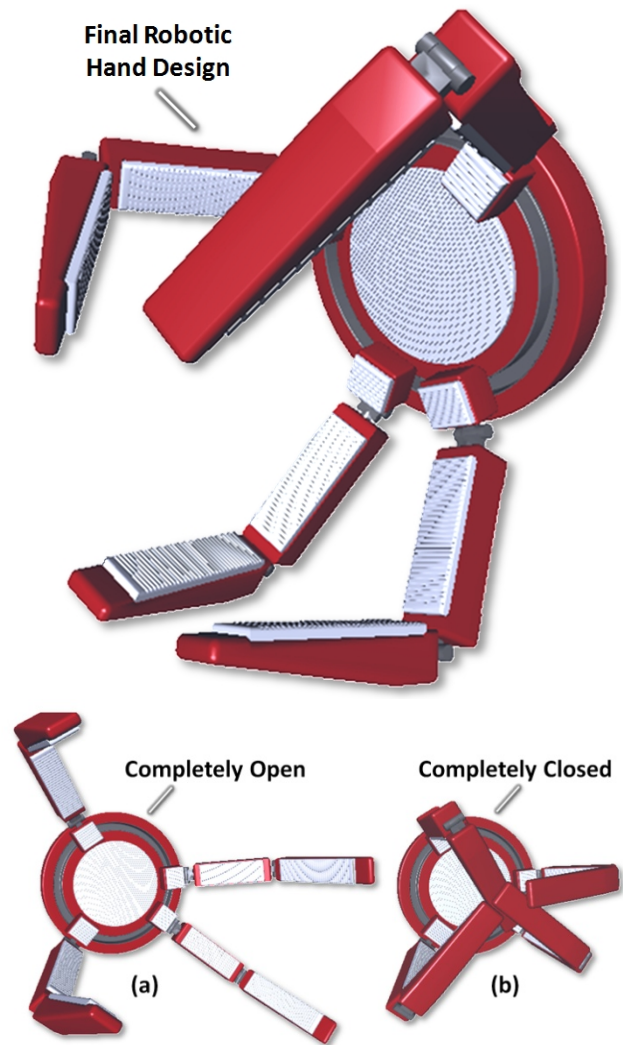

Fig. 6. Initial configuration of the final robotic hand design (top) along with completely open (a) and completely closed (b) hand configurations, corresponding to maximum motion range achievable from the initial configuration (top) given the new motion range limits (Table III). This figure only illustrates finger flexion DOFs, not abduction or rotation.
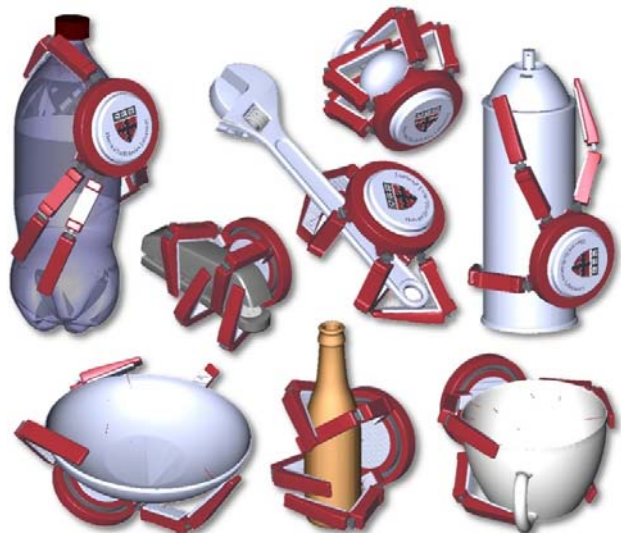

Fig. 7. The final robotic hand design acquiring representative object grasps. All grasp configurations conform to the joint angle limits in Table III.
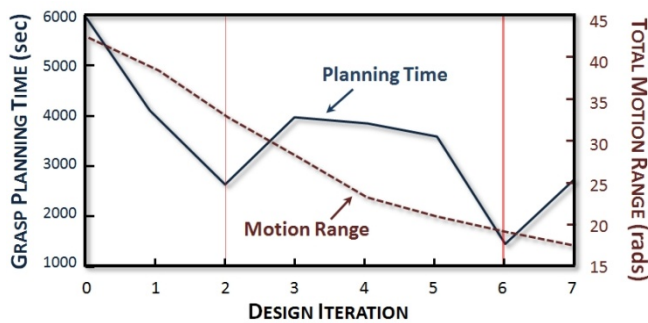
Fig. 8. Plot of average grasp planning time and aggregate motion range with respect to ATR design iteration. The vertical lines at design iterations two and six denote the elimination of robotic hand DOF.
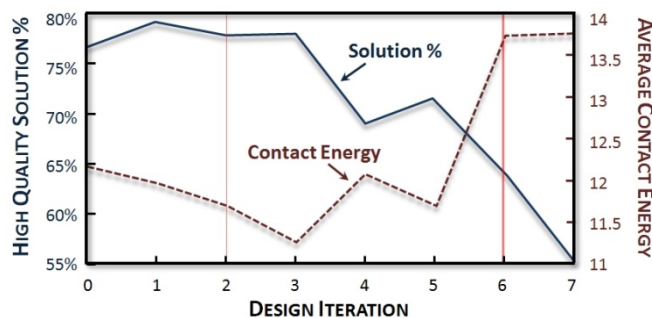

Fig.9. Plot of average hand contact energy and quality solution percentage with respect to ATR design iteration. The vertical lines at design iterations two and six denote the elimination of robotic hand DOF.

VI. DISCUSSION

The goal of this research is to propose and evaluate an actuation topology reduction (ATR) framework aimed at mitigating both the mechanical and the computational expense of implementing underactuated compliant robotic hand solutions without compromising grasp robustness. The results not only demonstrate the efficacy of the ATR framework but also provide insights into robotic hand design and illuminate areas for framework improvement.

A. Lessons from Framework Implementation

The ATR framework can be used to find joint coupling patterns or identify certain DOFs as candidates for passive compliance. Compliant joints, for example, could be assigned by motion range. DOFs with $\leq 30°$ of motion range (level 1) could, by default, be implemented using compliant joint flexures. For example, designing passive compliance into distal link twist DOF - rather than completely locking it - would eliminate the need for direct actuation but would allow for small perturbations that may promote better confirmation to objects with high curvature. Similarly, DOFs with $\geq 90°$ of motion range could be designed as fully actuated DOFs, as their importance to grasp robustness and large motion range warrant fine position and force control.

Principal component analysis (PCA) was performed on grasp solution data to identify DOF sets that can be driven by the same actuators and used as postural synergies grasp planning. The biplots of PCA data [23] in Fig. 10 show that our ATR framework produced a solution for which each

DOF makes a significant contribution to the achievement of grasp robustness. Ineffectual DOFs with minimal contribution to the principal component (PC) space were removed during topology reduction, resulting in PCs that span the solution set more efficiently.
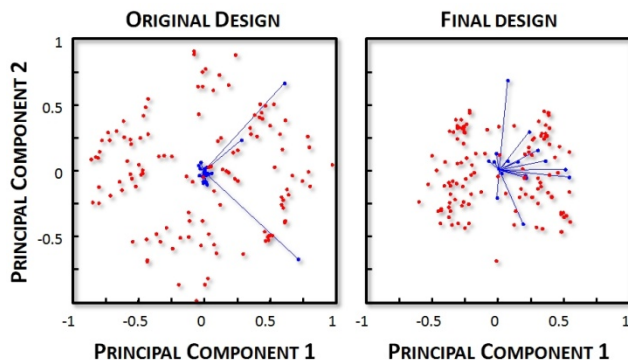

Fig. 10. Biplots of the first and second principal grasp components for the original and final robotic hand designs. Dots represent the location of grasp solutions in the PC space. Lines indicate the magnitude of each DOF's contribution to these PCs. The original design has only 3 DOFs with major contributions to the PCs; several have minimal contribution. A majority of the final design's DOFs have a significant contribution to the PCs.

The increased utility of each DOF in the reduced actuation topology, though desired for mechanical and computational cost benefits, also makes identifying DOFs for joint coupling more difficult. This is due to the facts that 1) each PC for the reduced actuation topology constitutes a smaller percentage of the PC space than for the original hand, and 2) most DOFs now have a significant contribution to each PC. If a DOF has a large coefficient in 3 PCs and each PC is driven by one motor, then this DOF would have to be coupled to 3 motors. This could complicate, rather than simplify, mechanical implementation. Despite this drawback, there are some DOFs, such as finger abduction, which can be coupled using PCA data (Fig 11).
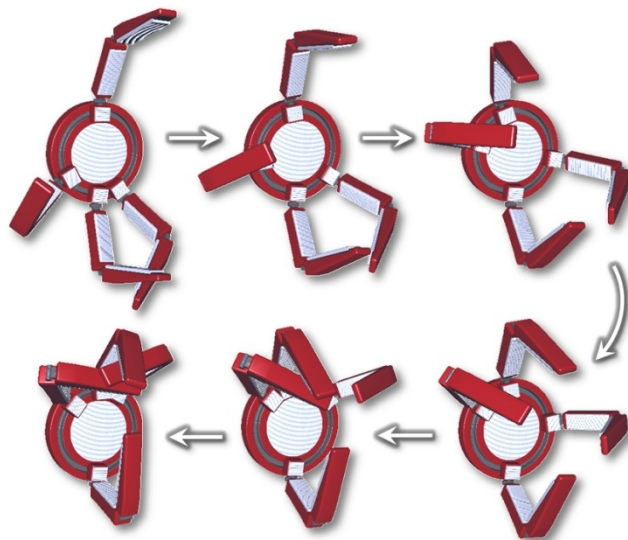

Fig. 11. First principal component of the final ATR robotic hand design. Abductions of the left and right finger are suitable for joint coupling.

B. Framework Improvements

The proposed method of actuation topology reduction is, like many design optimization problems, sensitive to problem formulation. The selection of parameters such as the initial hand configuration, design space variables, search methods, design rules, and cost functions have a significant impact on optimization results. The selection of a grasp quality metric is particularly important as it defines the space of 'reasonable' grasps for a given robotic hand. Using a grasp quality metric other than epsilon quality could lead to vastly disparate hand design solutions that, within the context of that new metric, are considered optimal but are sub-optimal with respect to other metrics.

Future work on ATR for robotic hand design will focus on the development of a systematic, non-arbitrary parameter selection method that preserves framework generality, and on a design protocol that places greater emphasis on joint coupling. Ideas along these lines include 1) predefined initial configurations, 2) adaptive grasp acquisition algorithms, 3) wrist posture constraints, 3) bidirectional, data-driven DOF modifications, 5) force-based pregrasp planning, and 6) PCA-based design evaluation at each ATR algorithm iteration. Efforts will also be made to study the sensitivity of the design optimization algorithm to grasp quality metrics in order to characterize and mitigate inherent solution biases.

VII. CONCLUSION AND FUTURE WORK

This paper presented an actuation topology reduction framework aimed at reducing the mechanical complexity and computational cost associated with dexterous robotic hands while maintaining acceptable grasp quality over a specific set of objects. This framework systematically demoted or removed DOFs from a robotic hand actuation topology according to their contribution to grasp quality. The resulting hand design contained fewer DOFs and a smaller configuration space than the original design, affording lower computational costs. Data-driven, heuristic assessment of DOF utility suggested potential kinematic locations for passively compliant joints, and principal component analysis yielded insights into candidate joint couples which further decrease system dimensionality.

This framework does not produce a definitive, universal solution for reduced or minimum complexity robotic hands but the results serve as a foundation for future research on the topic of hand design optimization. This research includes development of a more comprehensive graspable object set, the application of structured external wrenches to grasped objects to simulate intended use, and more a thorough treatment of contact mechanics, in particular force closure, for increased simulation fidelity. Related work will involve the optimization of robotic hand morphological parameters such as the number of fingers, finger link dimensions, and an exhaustive study of data-driven joint coupling methods.

REFERENCES

[1] S. Jacobsen, E. Iversen, D. Knutti, R. Johnson, and K. Biggers, "Design of the Utah/M.I.T. Dexterous Hand," *Proc. IEEE Int. Conf. Robotics and Automation*, San Francisco, CA, 1986, pp. 1520-1532.

[2] C. Lovchik and M. Dilfer, "The Robonaut Hand: A Dexterous Robot Hand for Space," *Proc. IEEE Int. Conf. Robotics and Intelligent Systems*, Detroit, MI, 1999, pp. 907-912.

[3] J. Butterfass, M. Grebenstein, H. Liu, and G. Hirzinger, "DLR-Hand II: next generation of a dexterous robot hand," *Proc. IEEE Int. Conf. Robotics and Automation*, Seoul, Korea, 2010, pp.109–114.

[4] M. C. Carrozza, G. Cappiello, S. Micera, B. B. Edin, L. Beccai, and C. Cipriani, "Design of a cybernetic hand for perception and action," *Biol. Cybern.*, vol. 95, no. 6, pp. 629–644, 2006.

[5] C. Brown and H. Asada, "Inter-finger coordination and postural synergies in robot hands via mechanical implementation of principal components analysis," *IEEE-RAS Int.Conf. on Intelligent Robots and Systems*, 2007, pp. 2877–2882.

[6] A. Dollar and R. Howe, "Simple, robust autonomous grasping in unstructured environments," *Proc. IEEE Int. Conf. on Robotics and Automation*, 2007, pp. 4693–4700.

[7] M. R. Cutkosky, "On grasp choice, grasp models, and the design of hands for manufacturing tasks," *IEEE Trans. on Robotics and Automation*, vol. 5, pp. 269–279, 1989.

[8] M. Santello, M. Flanders, and J. F. Soechting, "Postural Hand Synergies for Tool Use ," *The Journal of Neuroscience,* vol. 18, no. 23, pp. 10105-10115, Dec. 1998.

[9] M. Ciocarllie, C. Goldfeder, and P. Allen, "Dimensionality Reduction for hand-independent dexterous robotic grasping," *Proc. IEEE/RSJ Int. Conf. Robotics and Intelligent Sys.*, San Diego, CA, 2007, pp. 3270 – 3275.

[10] A. M. Dollar and R. D. Howe, "Joint Coupling Design of Underactuated Grippers," *Proc. of the 2006 Int. Design Engineering Technical Conf.* (IDETC), Philadelphia, PA, 2006.

[11] N. Pollard and R. Gilbert, "Tendon arrangement and muscle force requirements for humanlike force capabilities in a robotic finger," *IEEE Intl. Conf. on Robotics and Automation*, pp. 3755–3762, 2002.

[12] M. Ciocarlie and P. Allen, "A design and analysis tool for underactuated compliant hands," in *ISEEE-RSJ Int. Conf. on Intelligent Robots and Systems*, St. Louis, MO, 2009, pp. 1278 – 1283.

[13] A. T. Miller and P. K. Allen, "Graspit!: A Versatile Simulator for Robotic Grasping," *IEEE Robotics and Automation Magazine*, vol. 11, no.4, pp. 110-122, Dec. 2004.

[14] K. Matheus and A. M. Dollar, "Benchmarking grasping and manipulation: properties of the objects of daily living," *Proc. IEEE/RSJ Int. Conf. Robotics and Intelligent Systems*, Taipei, Taiwan, 2010, pp. 5020 –5027.

[15] K. B. Shimoga, "Robot grasp synthesis algorithms: a survey," *Intl. J. of Robotics Research*, vol. 15, pp. 230–266, 1996.

[16] C. Ferrari and J. Canny, "Planning Optimal Grasps," *Proc. IEEE Int. Conf. Robotics and Automation*, Nice, France, 2002, pp. 2290 – 2295.

[17] A. T. Miller and P. K. Allen, "Examples of 3D grasp quality computations," *Proc. IEEE Int. Conf. Robotics and Automation*, Detroit, Michigan, 1999, pp 1240–1246.

[18] J. Ponce and B. Faveqon, "On computing three- finger force closure grasps of polygonal objects," *IEEE Trans. on Robotics and Automation*, 1995.

[19] C. Borst, M. Fischer, and G. Hirzinger, "A fast and robust grasp planner for arbitrary 3D objects," *Proc. IEEE Int. Conf. on Robotics and Automation*, 1999, pp. 1890–1896.

[20] B. Mirtich and J. Canny. "Easily computable optimum grasps in 2-D and 3-D," *Proc. IEEE Int. Conf. on Robotics and Automation*, pp.739–747, 1994.

[21] M. Ciocarlie and P. K. Allen, "Hand Posture Subspaces for Dexterous Robotic Grasping," *Int. J. of Robotics Research*, vol. 28, 2009, pp. 851-867.

[22] R. Balasubramanian, L. Xu, P. D. Brook, J. R. Smith, and Y. Matsouka, "Human-Guided Grasp Measures Improve Grasp Robustness on Physical Robot," *Proc. IEEE Int. Conf. Robotics and Automation*, Anchorage, Alaska, 2010, pp. 2294 – 2301.

[23] I.T. Jolliffe, *Principal Component Analysis,* 2nd Ed. New York, NY: Springer, 1993, pp. 78–149.